Screening of a chemogenetic library unveils dual-stage antimalarials with low cytotoxicity

Laura Torres[a], Matthew E. Fishbaugher[b], Melanie Lam[a], Alexander T. Chao[b], Calla Martyn[c], Luying Pei[b], Debapriya Sengupta[b], Maxime Dauphinais[d], Jonathan E. Gable[b], Srinivasa P. S. Rao[b], Steffen Renner[e], W. Armand Guiguemde[b], Sebastian A. Mikolajczak[b], Anke Harupa[b#], Gabriel Mitchell[a#]

[a] Open Innovation at Global Health Disease Area, Biomedical Research, Novartis, Emeryville, CA, USA

[b] Global Health Disease Area, Biomedical Research, Novartis, Emeryville, CA, USA

[c] Discovery Sciences, Biomedical Research, Novartis, Emeryville, CA, USA

[d] Global Discovery Chemistry, Biomedical Research, Novartis, Emeryville, CA, USA

[e] Discovery Sciences, Biomedical Research, Novartis, Basel, Switzerland

[#]Corresponding authors: anke.harupa-chung@novartis.com and gabrielmitchell2@gmail.com

Running title: A screen unveils antimalarials with low cytotoxicity

ABSTRACT

The global effort to eradicate malaria requires the development of drugs with novel mechanisms of action and differentiated pharmacological profiles. Both liver and blood phases of *Plasmodium* infection are essential for disease progression and transmission, making them primary targets for therapeutic intervention. In this study, we established a dual-luciferase reporter assay to simultaneously assess *Plasmodium berghei* liver-stage development and host cell viability. Screening a library of bioactive small molecules with annotated human targets revealed several inhibitors with potent liver-stage activity and minimal cytotoxicity. Further profiling against *P. falciparum* asexual blood stages identified compounds with dual-stage activity, underscoring their potential utility for development as either prophylactic or therapeutic agents. Knowledge of their human targets will facilitate investigation into host- or parasite-directed antimalarial mechanisms, thereby accelerating both biological insight and rational drug development. Our findings constitute a valuable resource for research on malaria biology and the discovery of next-generation antimalarials.

KEYWORDS: *Plasmodium*, parasite, liver, blood, drug discovery, global health

INTRODUCTION

Malaria remains a global health challenge, affecting hundreds of millions annually and causing life-threatening complications, particularly in young children, pregnant women, travelers, and individuals with HIV (1). Most malaria cases are attributed to infection with *Plasmodium falciparum*, predominantly found in sub-Saharan Africa (1). However, *Plasmodium vivax* also accounts for a significant portion of malaria cases, exhibits a more widespread distribution, and causes clinical relapses (1, 2). *Plasmodium* parasites have repeatedly demonstrated their adaptability to environmental challenges and, despite the deployment of resources for antimalarial discovery, novel therapeutics are still required to face the emergence of drug resistance and support the global effort to eradicate malaria (3).

The complex lifecycle of *Plasmodium* provides several opportunities for therapeutic intervention (3, 4). Transmission begins when *Plasmodium* sporozoites are injected into humans by *Anopheles* mosquitoes. Shortly after the bite, sporozoites infiltrate the liver, where they invade hepatocytes and establish a parasitophorous vacuole, a specialized compartment that supports intracellular development by leveraging both host and parasite biological processes (5). Within this vacuole, parasites differentiate and replicate extensively via schizogony (5). In addition to forming replicative liver-stage schizonts, certain species such as *P. vivax* can produce hypnozoites. Hypnozoites are quiescent forms that persist for weeks to months before activating, leading to clinical relapses and continued transmission (2). Upon completion of liver-stage development, thousands of merozoites are released into the bloodstream, where they invade red blood cells and initiate the asexual replication cycle responsible for the symptomatic phase of malaria. A subset of these asexual blood-stage parasites differentiates into gametocytes, which

can be taken up by mosquitoes during a blood meal and complete sexual reproduction in the mosquito midgut (3, 6).

Although the liver phase is clinically silent, it is a critical bottleneck in the parasite lifecycle and an attractive target for chemoprevention. Liver-stage inhibitors can block the establishment of blood-stage infection, prevent symptom onset, and reduce transmission. Moreover, because parasite burden is low at this stage, liver-targeting compounds may carry a reduced risk of resistance development. Dual-stage inhibitors, which are active against both liver and asexual blood stages, offer additional flexibility, as they may be developed either as preventive agents or as treatments, depending on clinical needs and resistance management strategies (3, 4).

Phenotypic screening of compound libraries against *Plasmodium* parasites has been instrumental in antimalarial drug discovery (4). However, the largest and most comprehensive screens have focused on asexual blood stages (7-9), potentially biasing hit identification toward compounds that target blood stage-specific pathways (10-12). These screens typically involve testing large numbers of structurally diverse compounds, with only a minor fraction selected for subsequent medicinal chemistry optimization to improve potency, selectivity, and pharmacological properties, ultimately yielding molecules with robust in vivo efficacy (4, 13). Elucidating the mechanism of action for hits from phenotypic screens can be challenging, especially for compounds with a high barrier to resistance (14). However, once validated, biological targets can guide more focused drug discovery, a process that can be further accelerated through computational and structure-based approaches (4, 13).

In this study, we developed a dual-luciferase assay to rapidly assess both cytotoxicity and inhibitory activity of compounds against the liver stages of *P. berghei*, a model organism that causes malaria in rodents and readily infects human hepatoma cells (5, 15). Using this assay, we screened a library of bioactive compounds, including molecules with known mechanisms of action in human cells, and identified several hits with activity against *P. berghei* liver stages and minimal cytotoxicity. Some hits also inhibited *P. falciparum* asexual blood stages, suggesting either direct antiparasitic activity or the targeting of host pathways common to both hepatocytes and red blood cells. Other hits were only active against *P. berghei* liver stages, potentially acting on liver stage-specific host or parasite pathways. Overall, this study provides detailed information on novel compounds with antimalarial activity, including chemical structures and known human targets. These compounds represent promising starting points for the development of next-generation antimalarials.

MATERIALS AND METHODS

Cell culture

The human hepatoma Huh7 cell line (Japanese Collection of Research Bioresources (JCRB) Cell Bank) was grown in Dulbecco's Modified Eagle's Medium (DMEM) with high glucose (Gibco) supplemented with 10% heat-inactivated fetal bovine serum (FBS, Corning), 100 U/mL penicillin-streptomycin (Gibco) and 1% GlutaMAX™ (Gibco) (hereafter refer to as Huh7 medium) at 37 °C and 5% CO_2.

Generation of renilla luciferase-expressing Huh7 cells

Stable renilla luciferase-expressing Huh7 cells ($Huh7_{Rluc}$) were generated with lentivirus from BPS Bioscience (79565-G). Briefly, cells were transduced with a multiplicity of infection (MOI) of 2 in Huh7 medium containing 8 µg/mL of polybrene (AmericanBio) followed by centrifugation at 800 × g for 1 h at 37 °C, with low acceleration and break. One day post-transduction, lentiviruses were removed, and fresh cell culture media was added to cells. Transduced cells were then selected with 250 µg/mL of geneticin (G418) for 5 weeks.

P. berghei liver-stage infection assay

One day prior to infection, WT Huh7 or $Huh7_{Rluc}$ cells were seeded at a density of 8,000 cells per well in 384-well white solid bottom plate (Greiner, 781080). *Anopheles stephensi* mosquitoes infected with luciferase-expressing *P. berghei* ANKA strain GFP-$Luc_{ama1\text{-}eef1a}$ (Pb_{Fluc}) (16) were produced by the SporoCore (University of Georgia, UGA) and sporozoites were isolated by microdissection of salivary glands, as previously described with modifications (17, 18). Unless otherwise specified, cells were infected with 2,000 sporozoites per well in Roswell Park

Memorial Institute 1640 (RPMI, Gibco) medium containing 20% FBS (Corning). Infection was facilitated by centrifugation at 330 × *g* for 3 min at room temperature (RT), using low acceleration and braking settings. Cells were incubated with sporozoites for 2 h at 37 °C and 5% CO . The culture medium was then replaced with Huh7 medium, and compounds were added prior to further incubation for 48 hours under the same conditions.

Dual-luciferase reporter assay

The Dual-Glo® luciferase assay (Promega) was performed as specified by the provider with modifications. Briefly, media from cell cultures was replaced with 20 µL of Dual-Glo® luciferase reagent per well. Plates were incubated at RT for 10 min in the dark and shaken prior to measuring firefly luciferase (Fluc) luminescence signal. The Stop & Glo® buffer was then mixed 1:1 with DMEM without phenol red (Gibco) and 40 µL was added per well. Plates were then incubated at RT in the dark for 20 min and shaken prior to measuring the renilla luciferase (Rluc) luminescence signal. Luminescence signals were read using CLARIOstar® (BMG Labtech) or PHERAstar® FSX (BMG Labtech) plate readers.

Rluc assay

The Renilla-Glo® luciferase assay system (Promega) was used as specified by the provider with modifications. Briefly, $Huh7_{Rluc}$ cells were seeded at different concentrations in 384-well white solid bottom plate (Greiner) and incubated 1 day at 37°C and 5% CO_2. The cell culture media was then removed and replaced with 10 µL of Dulbecco's phosphate-buffer saline (D-PBS, Gibco) and 10 µL of Renilla-Glo® per well. Plates were shaken, incubated at RT in the dark for 10 minutes, and the luminescence signal was read using a CLARIOstar® plate reader.

ATP cell viability assay

Promega's CellTiter-Glo® 2.0 assay kit was used as specified by the provider with modifications. Briefly, 8,000 $Huh7_{Rluc}$ cells per well were seeded in 384-well white solid bottom plate (Greiner) and incubated 1 day at 37°C and 5% CO_2. Cells were then treated with compounds for two days, the cell culture media was replaced with 20 µL of CellTiter-Glo® reagent per well, plates were shaken and incubated at RT in the dark for 10 min, and the luminescence signal was read using a CLARIOstar® plate reader.

Screening of compounds against *P. berghei* using the dual-luciferase reporter assay

At two hours post-sporozoite infection, cell culture media was replaced, and samples were treated with a library of 6044 compounds at a final concentration of 10 µM using the Echo 650 Acoustic Liquid Handler (Beckman). This library comprises bioactive compounds with known human gene targets, including some compounds from the previously published Novartis Moa Box collection (19). Some but not all the information linked to this library is publicly accessible. Two days post-treatment, the dual-luciferase reporter assay was performed and luminescence signals were measured. Robust Z' (RZ') were calculated for each plates using luminescence signal values from DMSO-treated infected wells and DMSO-treated uninfected (Fluc) or empty (Rluc) wells. The data from plates with one or more RZ' below 0.2 were excluded. Percent activities were determined by normalizing the values of each well to DMSO-treated infected wells (0% inhibition) and DMSO-treated uninfected or empty wells (100% inhibition for Fluc and Rluc, respectively) and averaged for two to four independent experiments. For hit determination, the median values of DMSO-treated infected wells minus 4× (Fluc, threshold = -

84.24%) and 3× (Rluc, threshold = -41.64%) the robust standard deviations were applied as thresholds. Out of the 198 hits, 197 were further characterized - one compound was no longer available in the Novartis internal archive.

P. falciparum **asexual blood-stage assay**

P. falciparum 3D7 (BEI Resources, MRA-102) parasite cultures were grown with complete medium (RPMI 1640 medium (10.4 g/L) with 0.5% AlbuMAX II, 200 µM hypoxanthine, 50 mg/L gentamicin sulfate, 35 mM HEPES, 2.0 g/L sodium bicarbonate, and 11 mM glucose) and human erythrocytes at 37°C and 5% CO_2, as previously described (14). The antimalarial activity of compounds was measured according to a modified SYBR Green cell proliferation assay, as previously described (14).

Structural comparison of human ATR and *Plasmodium* proteins

A structural search was conducted to identify proteins similar to human ATR (UniProt ID Q13535; PDB ID 5YZ0) among all *P. falciparum* proteins using Foldseek (20) incorporated into UniProt (search parameters = AlphaFold/UniProt50v4 + PDB100 20240101, mode: 3Di/AA, taxonomic filter: *Plasmodium falciparum*, iterative search off). The top *P. falciparum* hit, an AlphaFold model for a phosphatidylinositol 4-kinase (PI(4)K, UniProt ID Q8I406), showed structural alignment between residues 1280-1556 and human ATR residues 2320-2632. The structural similarity between *Plasmodium* PI(4)$K_{1280-1556}$ and human $ATR_{2320-2632}$ was confirmed using PyMOL (RMSD, root mean square deviation: 1.832 Å; The PyMOL Molecular Graphics System, Version 3.1.3 Schrödinger, LLC).

PI(4)K enzymatic assay

A PI(4)K enzymatic assay was performed as previously described (21). Briefly, the assay was performed for 1h at RT in a 384-well black plate using the Transcreener ADP_2 FP detection kit (BellBrook) and a final assay volume of 10 µL containing 1nM of purified *P. vivax* PI(4)K protein, 10mM Tris, pH 7.5, 1mM DTT, 10 µM ATP, 5mM Mn^{2+}, 0.2% Triton X-100 and 11 µM L-α-phosphatidylinositol (dissolved in 3% *n*-octylglucoside). The reaction was then stopped by adding 10 µL of detection mix containing 1 × stop buffer, 4 nM AMP Alexa Fluor 633 tracer, and 20 µg/mL of ADP antibody. Fluorescence polarization measurements were performed on the Infinite M1000 plate reader (Tecan) with λ_{ex} = 635 nm and λ_{em}= 680 nm (bandwidth, 20 nm).

Compounds, dose response treatments and analyses

All compounds were obtained from the Novartis internal archive and resuspended in DMSO. For usual dose-response experiments, compounds from master plates, containing 7- to 10-points 3-fold or half-log serial dilution series, were transferred in assay plates using the mosquito® HV liquid handler (SPT Labtech), with maximal concentrations of 10 µM. Results were normalized (100%, DMSO-treated samples) and plotted with curve fitting on either GraphPad Prism (version 9.5) or DAVID Helios (version 3.2.0.364). For hit compounds, IC_{50} and CC_{50} values underwent transformation prior to medians, selectivity indexes (SIs), and IC_{50} *Pf* BS / IC_{50} *Pb* LS ratios determination (see Supplementary data S1). Briefly, data outside the limits of experimental detection were imputed to half the next lower or higher untested concentration, based on the serial dilution technic used for each assay. Subsequently, data were subjected to log10-transformation and median values were calculated. To compute SIs and IC_{50} *Pf* BS / IC_{50} *Pb* LS ratios, the data were reverted to their original scale. For accuracy, median values were re-

expressed along with their corresponding experimental detection limits. Numbers of technical replicates and independent experiments are indicated in Figure legends.

Annotation of hit compounds

Data for hit compounds were gathered from ChEMBL v35 (downloaded on 2024-12-01) and PubChem (downloaded on 2025-01-22). Target scores were determined as previously described (22).

Preparation of graphs and artworks

BioRender (biorender.com), GraphPad Prism (v9.5), ChemDraw Professional (v23.1.1.3) and Adobe Illustrator (v29.8.1) were used to create figures.

RESULTS

A dual-luciferase reporter assay for assessing *P. berghei* liver-stage development and host cell viability

A dual-luciferase assay was customized to simultaneously evaluate parasite growth and host cell viability during the liver phase of malaria infection (Fig. 1A). As a reporter of host cell viability, the renilla luciferase (Rluc) gene was introduced into Huh7 hepatoma cells via lentiviral transduction, yielding a luminescence signal that strongly correlated with cell number (Fig. S1A). These Rluc-expressing cells ($Huh7_{Rluc}$) were then infected with *P. berghei* sporozoites expressing the firefly luciferase (Fluc) gene (Pb_{Fluc}) (16) for a 2-day incubation period (Fig. 1A, step 1). Parasite and host signals were then quantified using the Dual-Glo® luciferase assay, which enables sequential measurement of Fluc (Fig. 1A, step 2) and Rluc (Fig. 1A, step 3) luminescence. Both signals were elevated by over two orders of magnitude compared to uninfected or untransduced controls (Fig. 1B-C). Moreover, the Fluc signal exhibited a strong positive correlation with the number of Pb_{Fluc} sporozoites used for infection (Fig. S1B), demonstrating the assay's sensitivity to parasite load.

To confirm the suitability of this assay for compound screening during liver-stage infection, we first tested three reference compounds: KDU691 (Fig. 1D), a known inhibitor of liver stages (21); chloroquine (Fig. 1E), which is active against asexual blood stages but not liver stages (23); and puromycin (Fig. 1F), a cytotoxic control compound. As anticipated, KDU691 reduced the Pb_{Fluc} signal with a half-maximal inhibitory concentration (IC_{50}) of 16.0 - 29.5 nM, consistent with previously reported values (21, 24), and showed no cytotoxicity toward $Huh7_{Rluc}$ cells, with a half-maximal cytotoxic concentration (CC_{50}) greater than 10,000 nM (Fig. 1D and S2D). Also

in line with expectations, chloroquine did not reduce either luminescence signal (Fig. 1E and S2F) (24), while puromycin affected both parasite and host cell signals (Fig. 1F and S2G) (see GNF-*Pf*-2016 in (25)). It is noteworthy that puromycin impacted Pb_{Fluc} at lower concentrations (IC_{50} = 231.0 - 319.3 nM) than $Huh7_{Rluc}$ (CC_{50} = 2994 - 3924 nM), possibly due to the faster replication rate of liver-stage parasites compared to that of host cells. Potency against Pb_{Fluc} was also in agreement with previously reported data for other established antimalarials, including cabamiquine (24, 26), atovaquone (24, 27, 28) and KAF179 (11) (Fig. S2). KAE609 showed only weak activity against *P. berghei* liver stages (IC_{50} = 4607 nM) (Fig. S2), consistent with earlier findings (11, 29) but contrasting with a recent report by Nguyen et al. (24). Notably, KAE609 showed minor cytotoxicity at higher concentrations, which may have contributed to the observed weak Pb_{Fluc} activity (Fig. S2). We further confirmed cell viability data for these antimalarials using an orthogonal assay (CellTiter-Glo®) that quantifies viable cells based on ATP levels (Fig. S2), and found that results were consistent across both assays. Overall, these results demonstrate that the dual-luciferase assay is a reliable and sensitive platform for evaluating compound activity against *P. berghei* liver stages and host cells.

Screening of a bioactive library against *P. berghei* liver stages using the dual-luciferase reporter assay

The dual-luciferase reporter assay was employed to screen a library of 6044 compounds, partially overlapping with the previously published Novartis Moa Box collection (19). This library consists of bioactive compounds with annotated human targets, sourced from both public and internal datasets. Compounds were screened at a final concentration of 10 μM across 2-4 independent experiments (Fig. 2A). As a quality control measure, robust Z' (RZ') values were

calculated for each plate and luminescence signal, and plates with RZ' values below 0.2 were excluded from further analysis (Fig. 2B). The means and standard deviations of RZ' for the Fluc and Rluc signals were 0.61 ± 0.21 and 0.76 ± 0.16, respectively, confirming the robustness and reliability of the assay. As expected from a bioactive collection, several compounds impacted liver-stage development and host cell viability (Fig. 2C). It is worth noting that some compounds induced an increase in the Rluc signal relative to DMSO-treated controls (Fig. 2C), likely reflecting a known technical artifact. Indeed, this effect is consistent with a previous report showing that certain compounds, including staurosporine, can enhance the activity of the CMV promoter (30), which drives Rluc expression in our system (Fig. S3). To select liver-stage inhibitors for follow-up studies, cutoffs were applied (see Materials and Methods), resulting in a set of 198 compounds with potent activity against *P. berghei* liver stages and minimal cytotoxicity (Fig. 2C). Together, these results demonstrate the utility of the dual-luciferase assay for compound screening. They also suggest that screening the bioactive library has led to the discovery of *Plasmodium* liver-stage inhibitors.

Dose-response validation of hit compounds against *P. berghei* liver stages

Compounds identified in the single-point screen were further validated through dose-response experiments using the dual-luciferase reporter assay (Fig. 3 and Supplementary data S1). These experiments enabled the determination of Pb_{Fluc} IC_{50}s (Fig. 3A), $\mathrm{Huh7}_{\mathrm{Rluc}}$ CC_{50}s (Fig. 3B) and selectivity indexes (SIs) (Fig. 3C), calculated as the ratio of CC_{50} to IC_{50}, which reflects the window between cytotoxicity and antimalarial activity. As a benchmark, the cytotoxic control compound puromycin yielded an SI of 9.4, which was used as an approximate cutoff for hit prioritization. Compounds were ranked by SI and visualized in a heat map, highlighting those

with potent activity against *P. berghei* liver stages (Fig. 3D). A total of 155 compounds exceeded an SI of 10 (Supplementary data S1), indicating selective antimalarial activity. For the majority of these hits, chemical structures and annotated mechanisms of action in human cells are publicly available (Supplementary data S1), which may facilitate downstream target identification (4, 7, 31, 32). Among the identified hits, several compounds have documented activity against asexual blood stages, including WR99210 (Hit # 5) (33, 34), LY-411575 (Hit # 7) (35), atovaquone (Hit # 9) (36, 37), pyrimethamine (Hit # 27) (7, 33), apicidin (Hit #32) (38), compound 3 / GNF-*Pf*-4076 (Hit #40) (25, 39), cycloguanil (Hit # 58) (7), and norketotifen (Hit # 59) (40) (Fig. 3D), suggesting that some of the newly identified compounds may possess multistage activity. Conversely, clomiphene (Hit # 47), a compound with previously reported liver stage-specific activity (32), was also among the identified hits (Fig. 3D). Overall, these results confirm that screening the bioactive library using the dual-luciferase reporter assay identified *Plasmodium* inhibitors.

Profiling hit compounds against *P. falciparum* asexual blood stages

Given that several identified hits have known activity against *Plasmodium* asexual blood stages (Fig. 3D), an expanded set of compounds was tested to assess cross-stage efficacy (Fig. 4 and Supplementary data S1). Notably, a subset of *P. berghei* liver-stage inhibitors also demonstrated activity against *P. falciparum* blood stages (Fig. 4A), resulting in a moderate positive correlation between liver-stage and blood-stage IC_{50}s ($r = 0.5309$) (Fig. 4B). Among compounds with an SI > 10, we identified 65 dual-stage (IC_{50} *Pf* BS / IC_{50} *Pb* LS < 10) and 55 potential liver stage-specific (IC_{50} *Pf* BS / IC_{50} *Pb* LS > 10) inhibitors (Fig. 4C, Supplementary data S1). These

findings suggest that a substantial fraction of the inhibitors target biological pathways essential for both liver-stage and asexual blood-stage development.

Conversely, compounds that exclusively inhibit *P. berghei* liver stages may act on host or parasite pathways uniquely required during liver-stage infection. Alternatively, they may exhibit species-specific activity across different *Plasmodium* parasites or constitute technical artifacts (41). Because the liver stage-specific inhibitors identified in this study are supported solely by data from the dual-luciferase reporter assay, further validation is required to confirm their biological relevance. Nevertheless, given the complementarity between the *P. berghei* liver-stage and the *P. falciparum* blood-stage assays, this study confidently identified a collection of dual-stage inhibitors of malaria.

Dual-stage inhibitors of *Plasmodium* parasites

The chemical structures and annotated human targets of several *Plasmodium* inhibitors highlighted in this study are publicly available (Supplementary data S1). Among the dual-stage inhibitors, notable examples include ATR inhibitors VE-822 and VE-821 (42, 43), a signal peptide peptidase-like 2A (SPPL2A) inhibitor (44), the γ-secretase and pan-Notch inhibitor Varegacestat (45), histone deacetylase (HDAC) inhibitors (Nanatinostat (46) and Hit # 31 (47)), the DNA topoisomerase I inhibitor Exatecan (48, 49), and a RabGGTase inhibitor (50, 51) (Fig. 5). While these compounds are known to act on host targets and pathways, their antimalarial activity may arise from the inhibition of *Plasmodium* homologs, particularly for validated parasite targets such as HDACs (38, 52) and DNA topoisomerases (53, 54). Moreover, knowledge of a compound's human target can facilitate the identification of structurally related

parasite proteins that may also be susceptible to inhibition. For example, we found that *P. falciparum* phosphatidylinositol 4-kinase (PI(4)K) (PF3D7_0509800) shares structural features with human ATR (Fig. S4). Consistent with this, ATR inhibitors VE-822 and VE-821 (Fig. 5) exhibit structural similarity to the known *Plasmodium* PI(4)K inhibitor MMV390048 (55) and potently inhibit recombinant *P. vivax* PI(4)K *in vitro* (Fig. S4). These findings suggest that our dual-stage inhibitors may exert antimalarial effects through parasite targets. Overall, this study has identified a diverse set of dual-stage antimalarial compounds, offering valuable starting points for target identification and therapeutic development.

DISCUSSION

The liver phase of *Plasmodium* infection represents a critical window for therapeutic intervention against malaria, complementing approaches targeting the symptomatic blood phase of infection (3, 4). During the liver phase, parasites undergo intracellular replication within hepatocytes, exploiting both host and parasite processes (5) that may be amenable to pharmacological modulation. However, effective liver-stage therapeutics must inhibit parasite development without significant adverse effects on host cells and tissues. To expedite the discovery of non-cytotoxic antimalarials, we tailored a dual-luciferase reporter assay capable of simultaneously quantifying *Plasmodium* liver-stage development and host cell viability, enabling immediate exclusion of cytotoxic compounds (Fig. 1). Using this assay, we screened a chemogenetic library of small molecules with annotated human targets (Fig. 2 and Supplementary data S1) and identified novel inhibitors of liver-stage parasites (Fig. 3). Several of these compounds also suppressed *P. falciparum* asexual blood stages (Fig. 4 and 5), suggesting dual-stage activity.

Although chemogenetic libraries provide a powerful approach for accelerating target identification (19, 56), dissecting compound mechanisms during liver-stage infection remains challenging. Homologous proteins in host and parasite can complicate target attribution and validation, particularly when phenotypes may arise from effects on either or both. However, our compounds that inhibit both liver and blood stages are hypothesized to act on parasite targets conserved across developmental stages and species, rather than on host pathways, as red blood cells lack nuclei and most organelles and therefore offer fewer host targets (57). For instance, Hit # 30 may inhibit *Plasmodium* RabGGTase (Fig. 5), potentially disrupting Rab protein prenylation and membrane localization (58, 59), suggesting that prenyltransferases may represent

a broader class of antimalarial targets (51, 60). As another example, human ATR inhibitors VE-822 and VE-821 may act on parasites by inhibiting *Plasmodium* PI(4)K (Fig. S4). These examples illustrate how annotated human targets, especially when integrated with structure-based approaches, can inform parasite target discovery and accelerate mechanistic insight.

In addition to dual-stage inhibitors, we also identified compounds with potential liver stage-specific activity. These may act on parasite pathways uniquely required for liver-stage development, on host pathways, or reflect species-specific biology, as liver-stage activity was assessed in *P. berghei* and blood-stage activity in *P. falciparum*. An example of a host-directed mechanism is the inhibition of liver stages by the cholesterol trafficking and biosynthesis inhibitor U18666A (61, 62) (Hit # 12, Supplementary data S1; (63)), consistent with the established role of host cholesterol in supporting parasite development (63, 64). Our results also suggest that liver-stage parasites may be sensitive to inhibition of host hypoxia-inducible factor (HIF)-1α (Moracin P, Hit #22; Supplementary data S1), a transcription factor mediating cellular responses to hypoxia in addition to its roles under normoxic conditions (65-67). Consistent with this finding, a previous study indicated that hypoxia promotes the development of *Plasmodium* liver stages through mechanisms partly mediated by HIF-1α (68). Interestingly, HIFs and the hepatic oxygen gradient have been implicated in the metabolic zonation of the liver (69), with the perivenous lobule zone—characterized by lower oxygen tension—being more permissive to liver-stage development (68, 70). As such, HIF-1α may contribute to the differential susceptibility of hepatocyte subpopulations to *Plasmodium* infection. Overall, these findings highlight potential host-parasite interactions that warrant further investigation.

The chemically diverse hits identified in this study broaden the antimalarial discovery space and include potent, low-toxicity inhibitors with structures and annotations that support mechanism-of-action deconvolution and medicinal chemistry optimization. Although further profiling is needed to assess their suitability, some compounds may serve as starting points for developing chemotypes with potential relevance to MMV's long-acting chemoprotection strategy (71). In summary, this study lays the groundwork for future efforts to validate novel targets, optimize lead compounds, and inform the design of next-generation antimalarial drugs for both prevention and treatment.

ACKNOWLEDGEMENTS

The authors thank Thomas Krucker and Thierry T. Diagana for providing their support and mentorship during the execution of this study. The authors also thank Harry Cheung, Allen Cornett, Richard T. Eastman, Erika L. Flannery, Rajiv S. Jumani, Eric J. Martin, Beat Nyfeler, Maude Patoor and Joseph M. Young for helpful discussions and technical assistance, and the SporoCore group (University of Georgia) for producing *P. berghei*-infected mosquitoes. This work was supported by a grant from the Gates Foundation (INV010720; Thierry T. Diagana). The conclusions and opinions expressed in this work are those of the authors alone and shall not be attributed to the Gates Foundation. All authors were employed by and/or shareholders of Novartis Pharma AG during this study.

AUTHOR CONTRIBUTIONS

Laura Torres: Conceptualization, Data curation, Formal analysis, Investigation, Methodology, Visualization, Writing - original draft. **Matthew E. Fishbaugher**: Investigation, Methodology. **Melanie Lam**: Investigation. **Alexander T. Chao**: Investigation, Data curation, Formal analysis. **Calla Martyn**: Formal analysis, Software. **Luying Pei**: Investigation, Data curation. **Debapriya Sengupta**: Investigation, Data curation. **Maxime Dauphinais**: Formal analysis, Visualization. **Jonathan E. Gable**: Formal analysis. **Srini P.S. Rao**: Conceptualization, Supervision. **Steffen Renner**: Conceptualization, Formal analysis, Software. **W. Armand Guiguemde**: Methodology, Supervision. **Sebastian A. Mikolajczak**: Conceptualization, Supervision. **Anke Harupa**: Conceptualization, Investigation, Methodology, Supervision, Writing - original draft. **Gabriel Mitchell**: Conceptualization, Formal analysis, Investigation, Methodology, Project

administration, Supervision, Visualization, Writing - original draft. **All authors**: Writing - review & editing.

REFERENCES

1. World Health Organization. 2024. World malaria report. World Health Organization, Geneva, Switzerland.
2. Schafer C, Zanghi G, Vaughan AM, Kappe SHI. 2021. Plasmodium vivax Latent Liver Stage Infection and Relapse: Biological Insights and New Experimental Tools. Annu Rev Microbiol 75:87–106.
3. Duffey M, Shafer RW, Timm J, Burrows JN, Fotouhi N, Cockett M, Leroy D. 2024. Combating antimicrobial resistance in malaria, HIV and tuberculosis. Nat Rev Drug Discov 23:461–479.
4. Siqueira-Neto JL, Wicht KJ, Chibale K, Burrows JN, Fidock DA, Winzeler EA. 2023. Antimalarial drug discovery: progress and approaches. Nat Rev Drug Discov 22:807–826.
5. Vaughan AM, Kappe SHI. 2017. Malaria Parasite Liver Infection and Exoerythrocytic Biology. Cold Spring Harb Perspect Med 7.
6. Cowman AF, Healer J, Marapana D, Marsh K. 2016. Malaria: Biology and Disease. Cell 167:610–624.
7. Plouffe D, Brinker A, McNamara C, Henson K, Kato N, Kuhen K, Nagle A, Adrián F, Matzen JT, Anderson P, Nam TG, Gray NS, Chatterjee A, Janes J, Yan SF, Trager R, Caldwell JS, Schultz PG, Zhou Y, Winzeler EA. 2008. In silico activity profiling reveals the mechanism of action of antimalarials discovered in a high-throughput screen. Proc Natl Acad Sci U S A 105:9059–64.
8. Guiguemde WA, Shelat AA, Bouck D, Duffy S, Crowther GJ, Davis PH, Smithson DC, Connelly M, Clark J, Zhu F, Jiménez-Díaz MB, Martinez MS, Wilson EB, Tripathi AK,

Gut J, Sharlow ER, Bathurst I, El Mazouni F, Fowble JW, Forquer I, McGinley PL, Castro S, Angulo-Barturen I, Ferrer S, Rosenthal PJ, Derisi JL, Sullivan DJ, Lazo JS, Roos DS, Riscoe MK, Phillips MA, Rathod PK, Van Voorhis WC, Avery VM, Guy RK. 2010. Chemical genetics of Plasmodium falciparum. Nature 465:311–5.

9. Gamo FJ, Sanz LM, Vidal J, de Cozar C, Alvarez E, Lavandera JL, Vanderwall DE, Green DV, Kumar V, Hasan S, Brown JR, Peishoff CE, Cardon LR, Garcia-Bustos JF. 2010. Thousands of chemical starting points for antimalarial lead identification. Nature 465:305–10.

10. Abraham M, Gagaring K, Martino ML, Vanaerschot M, Plouffe DM, Calla J, Godinez-Macias KP, Du AY, Wree M, Antonova-Koch Y, Eribez K, Luth MR, Ottilie S, Fidock DA, McNamara CW, Winzeler EA. 2020. Probing the Open Global Health Chemical Diversity Library for Multistage-Active Starting Points for Next-Generation Antimalarials. ACS Infect Dis 6:613–628.

11. Meister S, Plouffe DM, Kuhen KL, Bonamy GM, Wu T, Barnes SW, Bopp SE, Borboa R, Bright AT, Che J, Cohen S, Dharia NV, Gagaring K, Gettayacamin M, Gordon P, Groessl T, Kato N, Lee MC, McNamara CW, Fidock DA, Nagle A, Nam TG, Richmond W, Roland J, Rottmann M, Zhou B, Froissard P, Glynne RJ, Mazier D, Sattabongkot J, Schultz PG, Tuntland T, Walker JR, Zhou Y, Chatterjee A, Diagana TT, Winzeler EA. 2011. Imaging of Plasmodium liver stages to drive next-generation antimalarial drug discovery. Science 334:1372–7.

12. Antonova-Koch Y, Meister S, Abraham M, Luth MR, Ottilie S, Lukens AK, Sakata-Kato T, Vanaerschot M, Owen E, Jado JC, Maher SP, Calla J, Plouffe D, Zhong Y, Chen K, Chaumeau V, Conway AJ, McNamara CW, Ibanez M, Gagaring K, Serrano FN, Eribez

K, Taggard CM, Cheung AL, Lincoln C, Ambachew B, Rouillier M, Siegel D, Nosten F, Kyle DE, Gamo FJ, Zhou Y, Llinás M, Fidock DA, Wirth DF, Burrows J, Campo B, Winzeler EA. 2018. Open-source discovery of chemical leads for next-generation chemoprotective antimalarials. Science 362.

13. Rao SPS, Manjunatha UH, Mikolajczak S, Ashigbie PG, Diagana TT. 2023. Drug discovery for parasitic diseases: powered by technology, enabled by pharmacology, informed by clinical science. Trends in Parasitology 39:260–271.

14. Taft BR, Yokokawa F, Kirrane T, Mata AC, Huang R, Blaquiere N, Waldron G, Zou B, Simon O, Vankadara S, Chan WL, Ding M, Sim S, Straimer J, Guiguemde A, Lakshminarayana SB, Jain JP, Bodenreider C, Thompson C, Lanshoeft C, Shu W, Fang E, Qumber J, Chan K, Pei LY, Chen YL, Schulz H, Lim J, Abas SN, Ang X, Liu YG, Angulo-Barturen I, Jiménez-Díaz MB, Gamo FJ, Crespo-Fernandez B, Rosenthal PJ, Cooper RA, Tumwebaze P, Aguiar ACC, Campo B, Campbell S, Wagner J, Diagana TT, Sarko C. 2022. Discovery and Preclinical Pharmacology of INE963, a Potent and Fast-Acting Blood-Stage Antimalarial with a High Barrier to Resistance and Potential for Single-Dose Cures in Uncomplicated Malaria. Journal of Medicinal Chemistry 65:3798–3813.

15. Lam M, Probst A, Torres L, Lantigua AA, Fishbaugher ME, Kumar JR, Saldivia M, Torres A, Hegde S, Aleshnick M, Jennison C, Roberson SGH, Joyner CJ, Vaughan AM, Wilder BK, Manneville C, Flannery EL, Marcellin D, Nyfeler B, Thiel Z, Mikolajczak SA, Harupa A, Mitchell G. 2025. HaloPROTAC3 does not trigger the degradation of the halotagged parasitophorous vacuole membrane protein UIS4 during Plasmodium liver stage development. Sci Rep 15:18323.

16. Pathak AK, Shiau JC, Franke-Fayard B, Shollenberger LM, Harn DA, Kyle DE, Murdock CC. 2022. Streamlining sporozoite isolation from mosquitoes by leveraging the dynamics of migration to the salivary glands. Malar J 21:264.

17. Vanderberg JP, Gwadz RW. 1980. The Transmission by Mosquitoes of Plasmodia in the Laboratory, p 153–234. *In* Kreier JP (ed), Pathology, Vector Studies, and Culture doi:https://doi.org/10.1016/B978-0-12-426102-0.50010-5. Academic Press.

18. Maher SP, Bakowski MA, Vantaux A, Flannery EL, Andolina C, Gupta M, Antonova-Koch Y, Argomaniz M, Cabrera-Mora M, Campo B, Chao AT, Chatterjee AK, Cheng WT, Chuenchob V, Cooper CA, Cottier K, Galinski MR, Harupa-Chung A, Ji H, Joseph SB, Lenz T, Lonardi S, Matheson J, Mikolajczak SA, Moeller T, Orban A, Padin-Irizarry V, Pan K, Peneau J, Prudhomme J, Roesch C, Ruberto A, Sabnis SS, Saney CL, Sattabongkot J, Sereshki S, Suriyakan S, Ubalee R, Wang Y, Wasisakun P, Yin J, Popovici J, McNamara CW, Joyner C, Nosten FH, Witkowski B, Le Roch KG, Kyle DE. 2025. A drug repurposing approach reveals targetable epigenetic pathways in Plasmodium vivax hypnozoites. Elife 13.

19. Canham SM, Wang Y, Cornett A, Auld DS, Baeschlin DK, Patoor M, Skaanderup PR, Honda A, Llamas L, Wendel G, Mapa FA, Aspesi P, Labbé-Giguère N, Gamber GG, Palacios DS, Schuffenhauer A, Deng Z, Nigsch F, Frederiksen M, Bushell SM, Rothman D, Jain RK, Hemmerle H, Briner K, Porter JA, Tallarico JA, Jenkins JL. 2020. Systematic Chemogenetic Library Assembly. Cell Chemical Biology 27:1124–1129.

20. van Kempen M, Kim SS, Tumescheit C, Mirdita M, Lee J, Gilchrist CLM, Söding J, Steinegger M. 2024. Fast and accurate protein structure search with Foldseek. Nat Biotechnol 42:243–246.

21. McNamara CW, Lee MC, Lim CS, Lim SH, Roland J, Simon O, Yeung BK, Chatterjee AK, McCormack SL, Manary MJ, Zeeman AM, Dechering KJ, Kumar TS, Henrich PP, Gagaring K, Ibanez M, Kato N, Kuhen KL, Fischli C, Nagle A, Rottmann M, Plouffe DM, Bursulaya B, Meister S, Rameh L, Trappe J, Haasen D, Timmerman M, Sauerwein RW, Suwanarusk R, Russell B, Renia L, Nosten F, Tully DC, Kocken CH, Glynne RJ, Bodenreider C, Fidock DA, Diagana TT, Winzeler EA. 2013. Targeting Plasmodium PI(4)K to eliminate malaria. Nature 504:248–253.

22. Wang Y, Cornett A, King FJ, Mao Y, Nigsch F, Paris CG, McAllister G, Jenkins JL. 2016. Evidence-Based and Quantitative Prioritization of Tool Compounds in Phenotypic Drug Discovery. Cell Chem Biol 23:862–874.

23. Sahu T, Lambert L, Herrod J, Conteh S, Orr-Gonzalez S, Carter D, Duffy PE. 2015. Chloroquine neither eliminates liver stage parasites nor delays their development in a murine Chemoprophylaxis Vaccination model. Front Microbiol 6:283.

24. Nguyen GB, Cooper CA, McWhorter O, Sharma R, Elliot A, Ruberto A, Freitas R, Pathak AK, Kyle DE, Maher SP. 2024. Screening the Global Health Priority Box against Plasmodium berghei liver stage parasites using an inexpensive luciferase detection protocol. Malar J 23:357.

25. Gagaring K, Borboa R, Francek C, Chen Z, Buenviaje J, Plouffe D, Winzeler E, Brinker A, Diagana T, Taylor J, Glynne R, Chatterjee A, Kuhen K. 2010. Novartis-GNF Malaria Box. https://chembl.gitbook.io/chembl-ntd/.

26. Baragaña B, Hallyburton I, Lee MC, Norcross NR, Grimaldi R, Otto TD, Proto WR, Blagborough AM, Meister S, Wirjanata G, Ruecker A, Upton LM, Abraham TS, Almeida MJ, Pradhan A, Porzelle A, Luksch T, Martínez MS, Luksch T, Bolscher JM, Woodland

A, Norval S, Zuccotto F, Thomas J, Simeons F, Stojanovski L, Osuna-Cabello M, Brock PM, Churcher TS, Sala KA, Zakutansky SE, Jiménez-Díaz MB, Sanz LM, Riley J, Basak R, Campbell M, Avery VM, Sauerwein RW, Dechering KJ, Noviyanti R, Campo B, Frearson JA, Angulo-Barturen I, Ferrer-Bazaga S, Gamo FJ, Wyatt PG, Leroy D, Siegl P, Delves MJ, Kyle DE, et al. 2015. A novel multiple-stage antimalarial agent that inhibits protein synthesis. Nature 522:315–20.

27. Davies CS, Pudney M, Nicholas JC, Sinden RE. 1993. The novel hydroxynaphthoquinone 566C80 inhibits the development of liver stages of Plasmodium berghei cultured in vitro. Parasitology 106 (Pt 1):1–6.

28. Barata L, Houzé P, Boutbibe K, Zanghi G, Franetich JF, Mazier D, Clain J. 2016. Analysis of the Interaction between Atovaquone and Proguanil against Liver Stage Malaria Parasites. Antimicrobial Agents and Chemotherapy 60:4333–4335.

29. Zeeman AM, van Amsterdam SM, McNamara CW, Voorberg-van der Wel A, Klooster EJ, van den Berg A, Remarque EJ, Plouffe DM, van Gemert GJ, Luty A, Sauerwein R, Gagaring K, Borboa R, Chen Z, Kuhen K, Glynne RJ, Chatterjee AK, Nagle A, Roland J, Winzeler EA, Leroy D, Campo B, Diagana TT, Yeung BK, Thomas AW, Kocken CH. 2014. KAI407, a potent non-8-aminoquinoline compound that kills Plasmodium cynomolgi early dormant liver stage parasites in vitro. Antimicrob Agents Chemother 58:1586–95.

30. Svensson RU, Barnes JM, Rokhlin OW, Cohen MB, Henry MD. 2007. Chemotherapeutic agents up-regulate the cytomegalovirus promoter: implications for bioluminescence imaging of tumor response to therapy. Cancer Res 67:10445–54.

31. Godinez-Macias KP, Chen D, Wallis JL, Siegel MG, Adam A, Bopp S, Carolino K, Coulson LB, Durst G, Thathy V, Esherick L, Farringer MA, Flannery EL, Forte B, Liu T, Godoy Magalhaes L, Gupta AK, Istvan ES, Jiang T, Kumpornsin K, Lobb K, McLean KJ, Moura IMR, Okombo J, Payne NC, Plater A, Rao SPS, Siqueira-Neto JL, Somsen BA, Summers RL, Zhang R, Gilson MK, Gamo FJ, Campo B, Baragaña B, Duffy J, Gilbert IH, Lukens AK, Dechering KJ, Niles JC, McNamara CW, Cheng X, Birkholtz LM, Bronkhorst AW, Fidock DA, Wirth DF, Goldberg DE, Lee MCS, Winzeler EA. 2025. Revisiting the Plasmodium falciparum druggable genome using predicted structures and data mining. NPJ Drug Discov 2:3.

32. Derbyshire ER, Prudêncio M, Mota MM, Clardy J. 2012. Liver-stage malaria parasites vulnerable to diverse chemical scaffolds. Proc Natl Acad Sci U S A 109:8511–6.

33. Warhurst DC. 2002. Resistance to antifolates in Plasmodium falciparum, the causative agent of tropical malaria. Sci Prog 85:89–111.

34. Childs GE, Lambros C. 1986. Analogues of N-benzyloxydihydrotriazines: in vitro antimalarial activity against Plasmodium falciparum. Ann Trop Med Parasitol 80:177–81.

35. Harbut MB, Patel BA, Yeung BK, McNamara CW, Bright AT, Ballard J, Supek F, Golde TE, Winzeler EA, Diagana TT, Greenbaum DC. 2012. Targeting the ERAD pathway via inhibition of signal peptide peptidase for antiparasitic therapeutic design. Proc Natl Acad Sci U S A 109:21486–91.

36. Nixon GL, Moss DM, Shone AE, Lalloo DG, Fisher N, O'Neill PM, Ward SA, Biagini GA. 2013. Antimalarial pharmacology and therapeutics of atovaquone. J Antimicrob Chemother 68:977–85.

37. Painter HJ, Morrisey JM, Vaidya AB. 2010. Mitochondrial electron transport inhibition and viability of intraerythrocytic Plasmodium falciparum. Antimicrob Agents Chemother 54:5281–7.

38. Darkin-Rattray SJ, Gurnett AM, Myers RW, Dulski PM, Crumley TM, Allocco JJ, Cannova C, Meinke PT, Colletti SL, Bednarek MA, Singh SB, Goetz MA, Dombrowski AW, Polishook JD, Schmatz DM. 1996. Apicidin: a novel antiprotozoal agent that inhibits parasite histone deacetylase. Proc Natl Acad Sci U S A 93:13143–7.

39. Mueller R, Reddy V, Nchinda AT, Mebrahtu F, Taylor D, Lawrence N, Tanner L, Barnabe M, Eyermann CJ, Zou B, Kondreddi RR, Lakshminarayana SB, Rottmann M, Street LJ, Chibale K. 2020. Lerisetron Analogues with Antimalarial Properties: Synthesis, Structure-Activity Relationship Studies, and Biological Assessment. ACS Omega 5:6967–6982.

40. Milner E, Sousa J, Pybus B, Auschwitz J, Caridha D, Gardner S, Grauer K, Harris E, Hickman M, Kozar MP, Lee P, Leed S, Li Q, Melendez V, Moon J, Ngundam F, O'Neil M, Parriott S, Potter B, Sciotti R, Tangteung A, Dow GS. 2012. Ketotifen is an antimalarial prodrug of norketotifen with blood schizonticidal and liver-stage efficacy. Eur J Drug Metab Pharmacokinet 37:17–22.

41. Auld DS, Inglese J. 2004. Interferences with Luciferase Reporter Enzymes. *In* Markossian S, Grossman A, Baskir H, Arkin M, Auld D, Austin C, Baell J, Brimacombe K, Chung TDY, Coussens NP, Dahlin JL, Devanarayan V, Foley TL, Glicksman M, Gorshkov K, Grotegut S, Hall MD, Hoare S, Inglese J, Iversen PW, Lal-Nag M, Li Z, Manro JR, McGee J, Norvil A, Pearson M, Riss T, Saradjian P, Sittampalam GS, Tarselli

MA, Trask OJ, Jr., Weidner JR, Wildey MJ, Wilson K, Xia M, Xu X (ed), Assay Guidance Manual, Bethesda (MD).

42. Charrier JD, Durrant SJ, Golec JM, Kay DP, Knegtel RM, MacCormick S, Mortimore M, O'Donnell ME, Pinder JL, Reaper PM, Rutherford AP, Wang PS, Young SC, Pollard JR. 2011. Discovery of potent and selective inhibitors of ataxia telangiectasia mutated and Rad3 related (ATR) protein kinase as potential anticancer agents. J Med Chem 54:2320–30.

43. Gorecki L, Andrs M, Rezacova M, Korabecny J. 2020. Discovery of ATR kinase inhibitor berzosertib (VX-970, M6620): Clinical candidate for cancer therapy. Pharmacol Ther 210:107518.

44. Brandl T, Ehrhardt C, Epple R, Markert C, Rigollier P, Velcicky J. 2022. Compounds and compositions as SPPL2A inhibitors.WO2022058902A1.

45. Aung KL, El-Khoueiry AB, Gelmon K, Tran B, Bajaj G, He B, Chen T, Zhu L, Poojary S, Basak S, Qi Z, Spreafico A, Fischer BS, Desai J. 2018. A multi-arm phase I dose escalating study of an oral NOTCH inhibitor BMS-986115 in patients with advanced solid tumours. Invest New Drugs 36:1026–1036.

46. Moffat D, Patel S, Day F, Belfield A, Donald A, Rowlands M, Wibawa J, Brotherton D, Stimson L, Clark V, Owen J, Bawden L, Box G, Bone E, Mortenson P, Hardcastle A, van Meurs S, Eccles S, Raynaud F, Aherne W. 2010. Discovery of 2-(6-{[(6-fluoroquinolin-2-yl)methyl]amino}bicyclo[3.1.0]hex-3-yl)-N-hydroxypyrimidine-5-carboxamide (CHR-3996), a class I selective orally active histone deacetylase inhibitor. J Med Chem 53:8663–78.

47. Remiszewski SW, Sambucetti LC, Bair KW, Bontempo J, Cesarz D, Chandramouli N, Chen R, Cheung M, Cornell-Kennon S, Dean K, Diamantidis G, France D, Green MA, Howell KL, Kashi R, Kwon P, Lassota P, Martin MS, Mou Y, Perez LB, Sharma S, Smith T, Sorensen E, Taplin F, Trogani N, Versace R, Walker H, Weltchek-Engler S, Wood A, Wu A, Atadja P. 2003. N-hydroxy-3-phenyl-2-propenamides as novel inhibitors of human histone deacetylase with in vivo antitumor activity: discovery of (2E)-N-hydroxy-3-[4-[[(2-hydroxyethyl)[2-(1H-indol-3-yl)ethyl]amino]methyl]phenyl]-2-propenamide (NVP-LAQ824). J Med Chem 46:4609–24.

48. Jo U, Murai Y, Agama KK, Sun Y, Saha LK, Yang X, Arakawa Y, Gayle S, Jones K, Paralkar V, Sundaram RK, Van Doorn J, Vasquez JC, Bindra RS, Choi WS, Pommier Y. 2022. TOP1-DNA Trapping by Exatecan and Combination Therapy with ATR Inhibitor. Mol Cancer Ther 21:1090–1102.

49. Mitsui I, Kumazawa E, Hirota Y, Aonuma M, Sugimori M, Ohsuki S, Uoto K, Ejima A, Terasawa H, Sato K. 1995. A new water-soluble camptothecin derivative, DX-8951f, exhibits potent antitumor activity against human tumors in vitro and in vivo. Jpn J Cancer Res 86:776–82.

50. Stigter EA, Guo Z, Bon RS, Wu YW, Choidas A, Wolf A, Menninger S, Waldmann H, Blankenfeldt W, Goody RS. 2012. Development of selective, potent RabGGTase inhibitors. J Med Chem 55:8330–40.

51. Ochocki JD, Distefano MD. 2013. Prenyltransferase Inhibitors: Treating Human Ailments from Cancer to Parasitic Infections. Medchemcomm 4:476–492.

52. Andrews KT, Haque A, Jones MK. 2012. HDAC inhibitors in parasitic diseases. Immunol Cell Biol 90:66–77.

53. Rao SPS, Gould MK, Noeske J, Saldivia M, Jumani RS, Ng PS, René O, Chen YL, Kaiser M, Ritchie R, Francisco AF, Johnson N, Patra D, Cheung H, Deniston C, Schenk AD, Cortopassi WA, Schmidt RS, Wiedemar N, Thomas B, Palkar R, Ghafar NA, Manoharan V, Luu C, Gable JE, Wan KF, Myburgh E, Mottram JC, Barnes W, Walker J, Wartchow C, Aziz N, Osborne C, Wagner J, Sarko C, Kelly JM, Manjunatha UH, Mäser P, Jiricek J, Lakshminarayana SB, Barrett MP, Diagana TT. 2023. Cyanotriazoles are selective topoisomerase II poisons that rapidly cure trypanosome infections. Science 380:1349–1356.

54. Dar A, Godara P, Prusty D, Bashir M. 2024. Plasmodium falciparum topoisomerases: Emerging targets for anti-malarial therapy. Eur J Med Chem 265:116056.

55. Paquet T, Le Manach C, Cabrera DG, Younis Y, Henrich PP, Abraham TS, Lee MCS, Basak R, Ghidelli-Disse S, Lafuente-Monasterio MJ, Bantscheff M, Ruecker A, Blagborough AM, Zakutansky SE, Zeeman AM, White KL, Shackleford DM, Mannila J, Morizzi J, Scheurer C, Angulo-Barturen I, Martínez MS, Ferrer S, Sanz LM, Gamo FJ, Reader J, Botha M, Dechering KJ, Sauerwein RW, Tungtaeng A, Vanachayangkul P, Lim CS, Burrows J, Witty MJ, Marsh KC, Bodenreider C, Rochford R, Solapure SM, Jiménez-Díaz MB, Wittlin S, Charman SA, Donini C, Campo B, Birkholtz LM, Hanson KK, Drewes G, Kocken CHM, Delves MJ, Leroy D, Fidock DA, et al. 2017. Antimalarial efficacy of MMV390048, an inhibitor of Plasmodium phosphatidylinositol 4-kinase. Sci Transl Med 9.

56. Jones LH, Bunnage ME. 2017. Applications of chemogenomic library screening in drug discovery. Nat Rev Drug Discov 16:285–296.

57. Chatzinikolaou PN, Margaritelis NV, Paschalis V, Theodorou AA, Vrabas IS, Kyparos A, D'Alessandro A, Nikolaidis MG. 2024. Erythrocyte metabolism. Acta Physiol (Oxf) 240:e14081.

58. Gisselberg JE, Zhang L, Elias JE, Yeh E. 2017. The Prenylated Proteome of Plasmodium falciparum Reveals Pathogen-specific Prenylation Activity and Drug Mechanism-of-action. Mol Cell Proteomics 16:S54–s64.

59. Suazo KF, Schaber C, Palsuledesai CC, Odom John AR, Distefano MD. 2016. Global proteomic analysis of prenylated proteins in Plasmodium falciparum using an alkyne-modified isoprenoid analogue. Sci Rep 6:38615.

60. Eastman RT, Buckner FS, Yokoyama K, Gelb MH, Van Voorhis WC. 2006. Thematic review series: lipid posttranslational modifications. Fighting parasitic disease by blocking protein farnesylation. J Lipid Res 47:233–40.

61. Long T, Hassan A, Thompson BM, McDonald JG, Wang J, Li X. 2019. Structural basis for human sterol isomerase in cholesterol biosynthesis and multidrug recognition. Nat Commun 10:2452.

62. Lu F, Liang Q, Abi-Mosleh L, Das A, De Brabander JK, Goldstein JL, Brown MS. 2015. Identification of NPC1 as the target of U18666A, an inhibitor of lysosomal cholesterol export and Ebola infection. Elife 4.

63. Petersen W, Stenzel W, Silvie O, Blanz J, Saftig P, Matuschewski K, Ingmundson A. 2017. Sequestration of cholesterol within the host late endocytic pathway restricts liver-stage Plasmodium development. Mol Biol Cell 28:726–735.

64. Labaied M, Jayabalasingham B, Bano N, Cha SJ, Sandoval J, Guan G, Coppens I. 2011. Plasmodium salvages cholesterol internalized by LDL and synthesized de novo in the liver. Cell Microbiol 13:569–86.

65. Majmundar AJ, Wong WJ, Simon MC. 2010. Hypoxia-inducible factors and the response to hypoxic stress. Mol Cell 40:294–309.

66. Knight M, Stanley S. 2019. HIF-1α as a central mediator of cellular resistance to intracellular pathogens. Curr Opin Immunol 60:111–116.

67. McGettrick AF, O'Neill LAJ. 2020. The Role of HIF in Immunity and Inflammation. Cell Metab 32:524–536.

68. Ng S, March S, Galstian A, Hanson K, Carvalho T, Mota MM, Bhatia SN. 2014. Hypoxia promotes liver-stage malaria infection in primary human hepatocytes in vitro. Dis Model Mech 7:215–24.

69. Kietzmann T. 2017. Metabolic zonation of the liver: The oxygen gradient revisited. Redox Biol 11:622–630.

70. Afriat A, Zuzarte-Luís V, Bahar Halpern K, Buchauer L, Marques S, Chora ÂF, Lahree A, Amit I, Mota MM, Itzkovitz S. 2022. A spatiotemporally resolved single-cell atlas of the Plasmodium liver stage. Nature 611:563–569.

71. El Gaaloul M, Tchouatieu AM, Kayentao K, Campo B, Buffet B, Ramachandruni H, Ndiaye JL, Wells TNC, Audibert C, Achan J, Donini C, Barsosio HC, Tinto H. 2024. Chemoprevention of malaria with long-acting oral and injectable drugs: an updated target product profile. Malar J 23:315.

FIGURE LEGENDS

Figure 1. A dual-luciferase reporter assay for simultaneous assessment of *P. berghei* liver-stage development and host cells viability. (A) Schematic overview of the dual-luciferase reporter assay. (Step 1) Renilla luciferase (Rluc)-expressing Huh7 ($Huh7_{Rluc}$) cells were infected with firefly luciferase (Fluc)-expressing *P. berghei* (Pb_{Fluc}) and incubated for 2 days prior measuring (Step 2) Pb_{Fluc} and (Step 3) $Huh7_{Rluc}$ luminescence. Fluc (B) and Rluc (C) luminescence of WT Huh7 and $Huh7_{Renilla}$ cells infected with Pb_{Fluc} for 2 days. Results are unnormalized and presented as means and SDs from one experiment with 5 technical replicates (n=5). Dose-response effect of the liver-stage inhibitor KDU691 (D), the blood-stage inhibitor chloroquine (E), and the cytotoxic control puromycin (F) on Fluc and Rluc luminescence signals. Half-maximal inhibitory concentration (IC_{50}) and half-maximal cytotoxic concentration (CC_{50}) values are shown for each compound. Data are normalized and expressed as means and SEMs from 4 independent experiments (N=4, with technical duplicates). 100% corresponds to DMSO-treated infected samples.

Figure 2. Screening of a chemogenetic library against *P. berghei* liver stages using the dual-luciferase reporter assay. (A) Diagram outlining the screening methodology. $Huh7_{Rluc}$ cells were seeded in 384-well plates, infected with firefly luciferase-expressing *P. berghei* (Pb_{Fluc}) sporozoites for 2h, treated with 10 μM of each compound using an acoustic liquid handler, and incubated for a total of 2 days prior to performing the dual-luciferase reporter assay. The impact of each compound was assessed across 2-4 independent experiments (N=2-4). (B) Robust Z' (RZ') were calculated for each plate and for both firefly luciferase (Fluc, in green) and renilla luciferase (Rluc, in blue) luminescence readouts. Plates with at least one RZ' value below 0.2

(gray dashed line) were excluded from further analysis. (C) Fluc and Rluc luminescence values associated with each compound. Data are normalized and presented as mean values. 0% (black dashed line) and -100% correspond to no and complete inhibition, respectively. Green dashed lines indicate the Fluc and Rluc luminescence thresholds for the determination of hits, with compounds in the green shaded area selected for further characterization.

Figure 3. Dose-response validation of hit compounds against *P. berghei* liver stages. The dose-response activity of hit compounds was assessed against *P. berghei* liver stages at 2 days post-infection using the dual-luciferase reporter assay. Median IC_{50}s (A), median CC_{50}s (B) and approximative selectivity indexes (SIs) (C) were determined from 2-4 independent experiments (N=2-4). Cabamiquine (in green) and puromycin (in blue) served as antimalarial and cytotoxic controls, respectively. Limits of detection are illustrated by grey dashed lines. Values below or above the limit of detection were imputed to allow the determination of medians and SIs. (D) Heat map illustrating median IC_{50}s and CC_{50}s for hit compounds. Compounds are organized from top to bottom based on their SI. Molecular structures of compounds with known antimalarial activity are showcased. Some data are shared between Fig. 3-5.

Figure 4. Characterization of hit compounds against *P. falciparum* asexual blood stages. (A) Heat map displaying median IC_{50}s of hit compounds against *P. berghei* (*Pb*) liver stages (LS) and *P. falciparum* (*Pf*) blood stages (BS). (B) Graph showing the correlation between *P. berghei* liver-stage and *P. falciparum* blood-stage IC_{50}s. Median IC_{50}s against *P. falciparum* blood stages were obtained from at least one experiment with technical duplicates. The Pearson correlation coefficient (*r*) is shown. Values outside the limits of detection were imputed to calculate medians

and harmonized between assays for graphical representation. (C) Venn diagram showing numbers of compounds with dual-stage (IC_{50} *Pf* BS / IC_{50} *Pb* LS < 10) and liver stage-specific (IC_{50} *Pf* BS / IC_{50} *Pb* LS > 10) antimalarial activities. Only compounds with an SI (CC_{50} Huh7 / IC_{50} *Pb* LS > 10) were considered. Some data are shared between Fig. 3-5.

Figure 5. Dual-stage inhibitors of *Plasmodium* parasites. Structures of select dual-stage inhibitors are featured. Primary known mechanism of action in human and ranges of IC_{50}s (i.e., min - max nM values) against *P. berghei* (*Pb*) liver stages (LS) and *P. falciparum* (*Pf*) asexual blood stages (BS) are shown. Compounds were selected based on their antimalarial activities and the absence of detectable cytotoxicity in $Huh7_{Rluc}$ cells (CC_{50} > 10000 nM). Results are from at least two independent experiments (N=2). ATR, ataxia telangiectasia and Rad3-related; HDAC, histone deacetylase; RabGGTase, Rab geranylgeranyl-transferase; SPPL2A, signal peptide peptidase-like 2A. * indicates that one outlier value was excluded from the corresponding IC_{50} range. Some data are shared between Fig. 3-5.

ADDITIONAL FILES

Figure S1. (A) Renilla luminescence (Rluc) as of function of the number of $Huh7_{Rluc}$ cells seeded per well of a 384-well plate. Results were obtained from uninfected cells, using the Rluc assay, and are represented as means and SDs from one experiment (N=1) performed with six technical replicates. (B) Firefly luciferase (Fluc) luminescence as of function of the number of Fluc-expressing *P. berghei* (Pb_{Fluc}) sporozoites used to infect cells for 2 days. Results were obtained using the dual-luciferase reporter assay and are represented as means and SDs from one experiment (N=1) performed with four technical replicates. Coefficients of determination (R^2) from simple linear regressions are shown.

Figure S2. Dose-response graphs showing the impact of cabamiquine (A), atovaquone (B), KAF179 (C), KDU691 (D), KAE609 (E), chloroquine (F) and puromycin (G) on *P. berghei* (Pb_{Fluc}) liver-stage development and Huh7 ($Huh7_{Rluc}$) viability as determined using the dual-luciferase reporter assay 2 days post-infection. The toxicity of compounds was also assessed in uninfected cells using the CellTiter-Glo® (CTG) assay. Results are presented as means and SEMs from 3-4 independent experiments (N =3-4) performed with 2-4 technical replicates. IC_{50}s (Pb_{Fluc}) and CC_{50}s ($Huh7_{Rluc}$ and $Huh7_{CTG}$) are shown above each graph. 100% corresponds to DMSO-treated samples. Some data are shared between Fig. 1 and Fig. S2.

Figure S3. Dose-response graph showing the effect of staurosporine on *P. berghei* (Pb_{Fluc}) liver-stage development and Huh7 ($Huh7_{Rluc}$) viability as determined using the dual-luciferase reporter assay 2 days post-infection. The toxicity of compounds was also determined in uninfected cells using the CellTiter-Glo® (CTG) assay. Results are presented as means and SEMs from 3-4

independent experiments (N=3-4) performed with technical duplicates. 100% corresponds to DMSO-treated samples.

Figure S4. (A) Structural alignment of *P. falciparum* PI(4)K (amino acid 1280-1556, in pink) and human ATR (amino acid 2320-2632, in blue). The alignment was performed using PyMol as described in the Materials and Methods. RMSD, root mean square deviation. (B) Effect of ATR inhibitors VE-822 (Hit #14) and VE-821 (Hit #37) and a control *Plasmodium* PI(4)K inhibitor (MMV390048) on the activity of recombinant *P. vivax* (Pv) PI(4)K. Results are presented as means and SDs from one experiment (N=1) performed with technical duplicates. IC_{50}s are shown. 100% corresponds to DMSO-treated samples.

Supplementary data S1. (Summary table sheet) InChIKey, preferred name(s), top human target, mean single-point activity (%) against *P. berghei* (Pb_{Fluc}) liver stages (LS) and $Huh7_{Rluc}$, median Pb_{Fluc} LS IC_{50}s and $Huh7_{Rluc}$ CC_{50}s, SIs, and median *P. falciparum* asexual blood-stage (BS) IC_{50}s for hit compounds. Only publicly available information is listed, except for the profiling of antimalarial activities. (Cmpd characteristics sheet) InChIKey, ChEMBL IDs, compound ID (CID) number and PubChem names for hit compounds. Only publicly available information is listed. (Human cmpd target sheet) Human targets, including the target with best score, for hit compounds. Only publicly available information is listed. (*Pb* LS dual luciferase) Raw and transformed data for the dose-response effect of hit compounds on Pb_{Fluc} LS and $Huh7_{Rluc}$ cells. (*Pf* BS sheet) Raw and transformed data for the dose-response effect of hit compounds on *P. falciparum* BS. (LS vs dual-stage sheet) List of compounds with LS-specific (IC_{50} *Pf* BS / IC_{50}

Pb LS > 10) and dual-stage (IC_{50} *Pf* BS / IC_{50} *Pb* LS < 10) activity. Only compounds with a SI (CC_{50} Huh7 / IC_{50} *Pb* LS) > 10 were included.

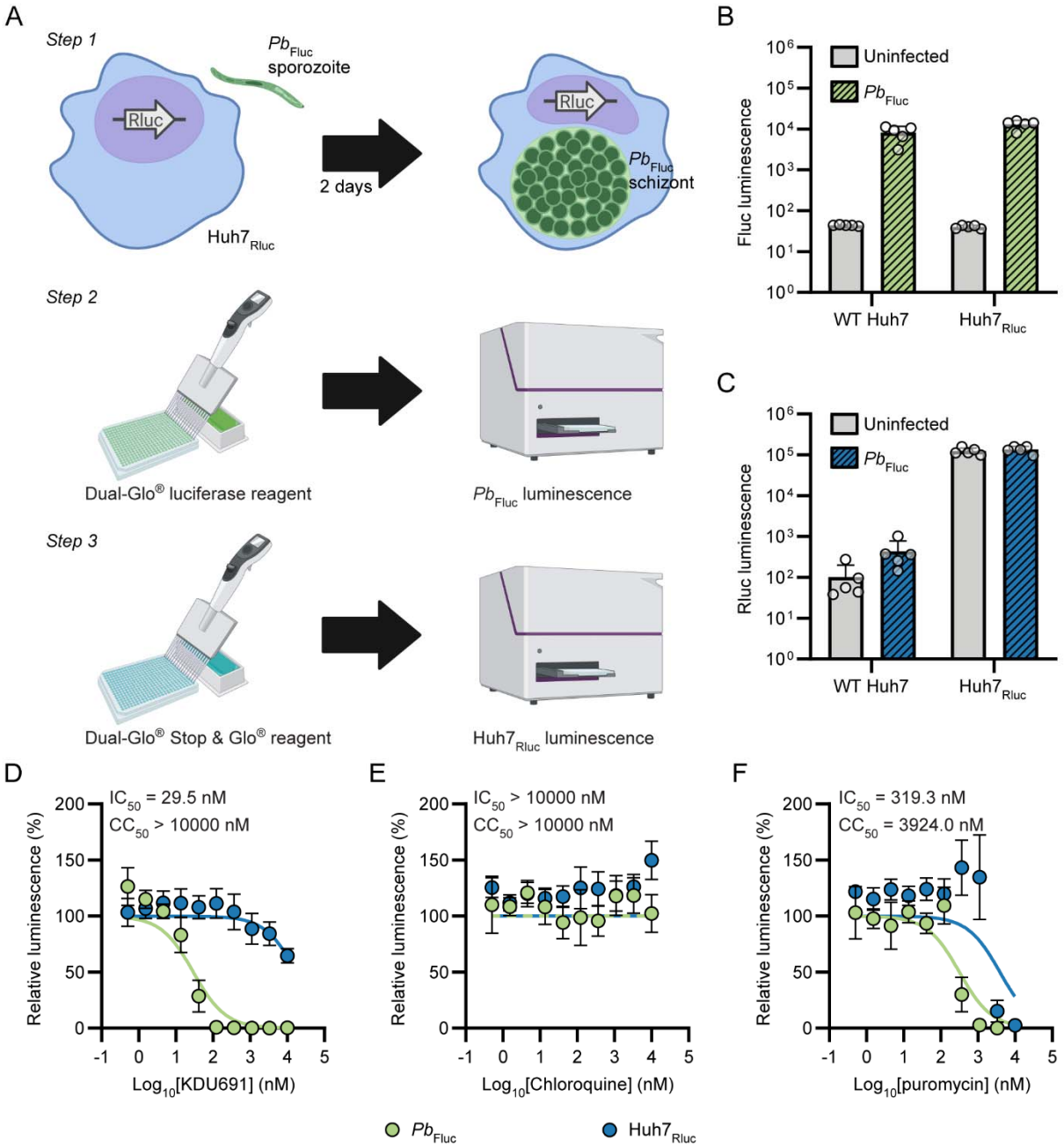
A
Step 1
Pb Fluc sporozoite
Rluc
Huh7 Rluc
2 days
Pb Fluc schizont
Step 2
Dual-Glo® luciferase reagent
Pb Fluc luminescence
Step 3
Dual-Glo® Stop & Glo® reagent
Huh7 Rluc luminescence
B
Uninfected
Pb Fluc
Fluc luminescence
WT Huh7
Huh7 Rluc
C
Rluc luminescence
D
IC50 = 29.5 nM
CC50 > 10000 nM
Relative luminescence (%)
Log10[KDU691] (nM)
E
IC50 > 10000 nM
CC50 > 10000 nM
Log10[Chloroquine] (nM)
F
IC50 = 319.3 nM
CC50 = 3924.0 nM
Log10[puromycin] (nM)

FIGURE 1.

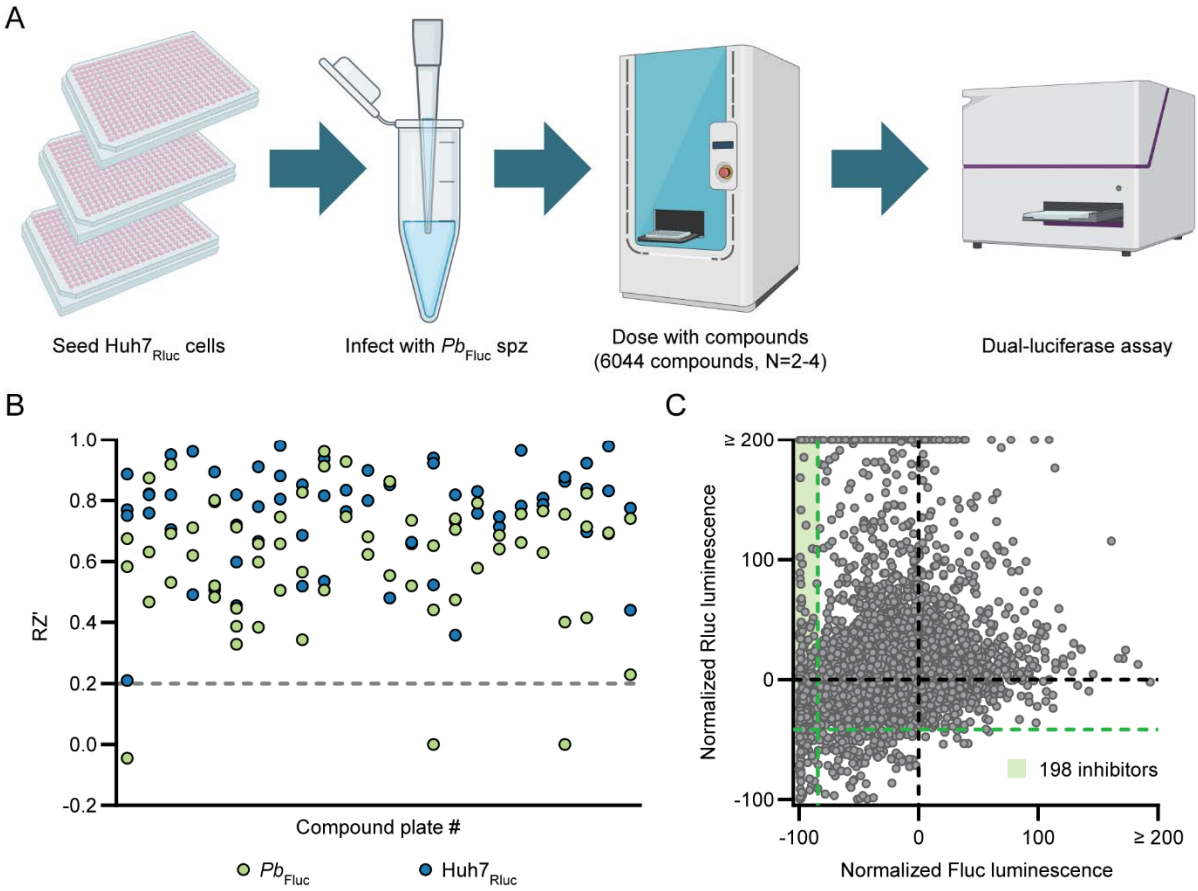
A
Seed Huh7Rluc cells
Infect with PbFluc spz
Dose with compounds
(6044 compounds, N=2-4)
Dual-luciferase assay
B
RZ'
1.0
0.8
0.6
0.4
0.2
0.0
-0.2
Compound plate #
PbFluc
Huh7Rluc
C
Normalized Rluc luminescence
≥ 200
100
0
-100
198 inhibitors
-100
0
100
≥ 200
Normalized Fluc luminescence

FIGURE 2.

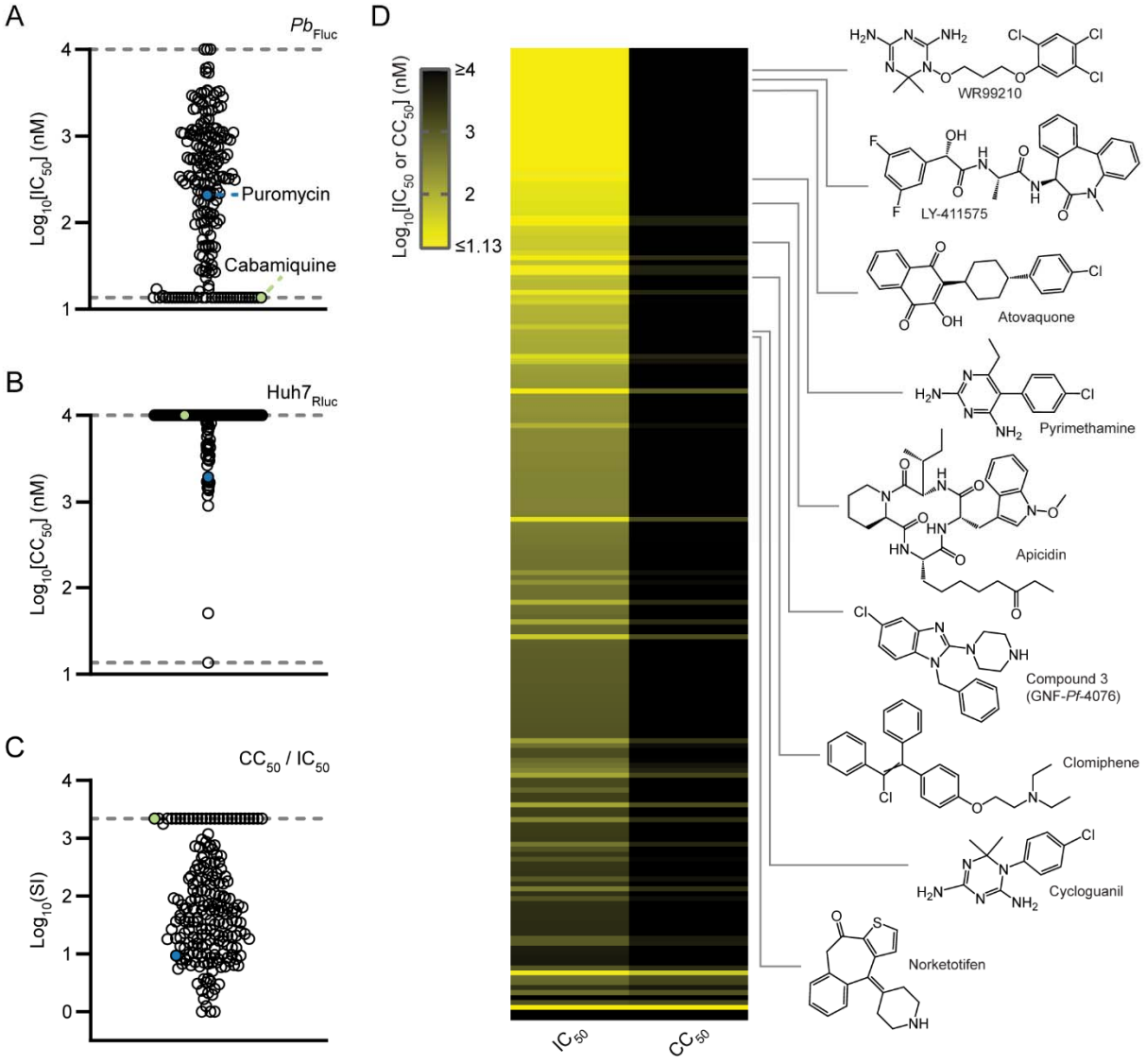
A
Pb Fluc
Log10[IC50] (nM)
Puromycin
Cabamiquine
B
Huh7 Rluc
Log10[CC50] (nM)
C
CC50 / IC50
Log10(SI)
D
Log10[IC50 or CC50] (nM)
≥4
3
2
≤1.13
IC50
CC50
WR99210
LY-411575
Atovaquone
Pyrimethamine
Apicidin
Compound 3
(GNF-Pf-4076)
Clomiphene
Cycloguanil
Norketotifen

FIGURE 3.

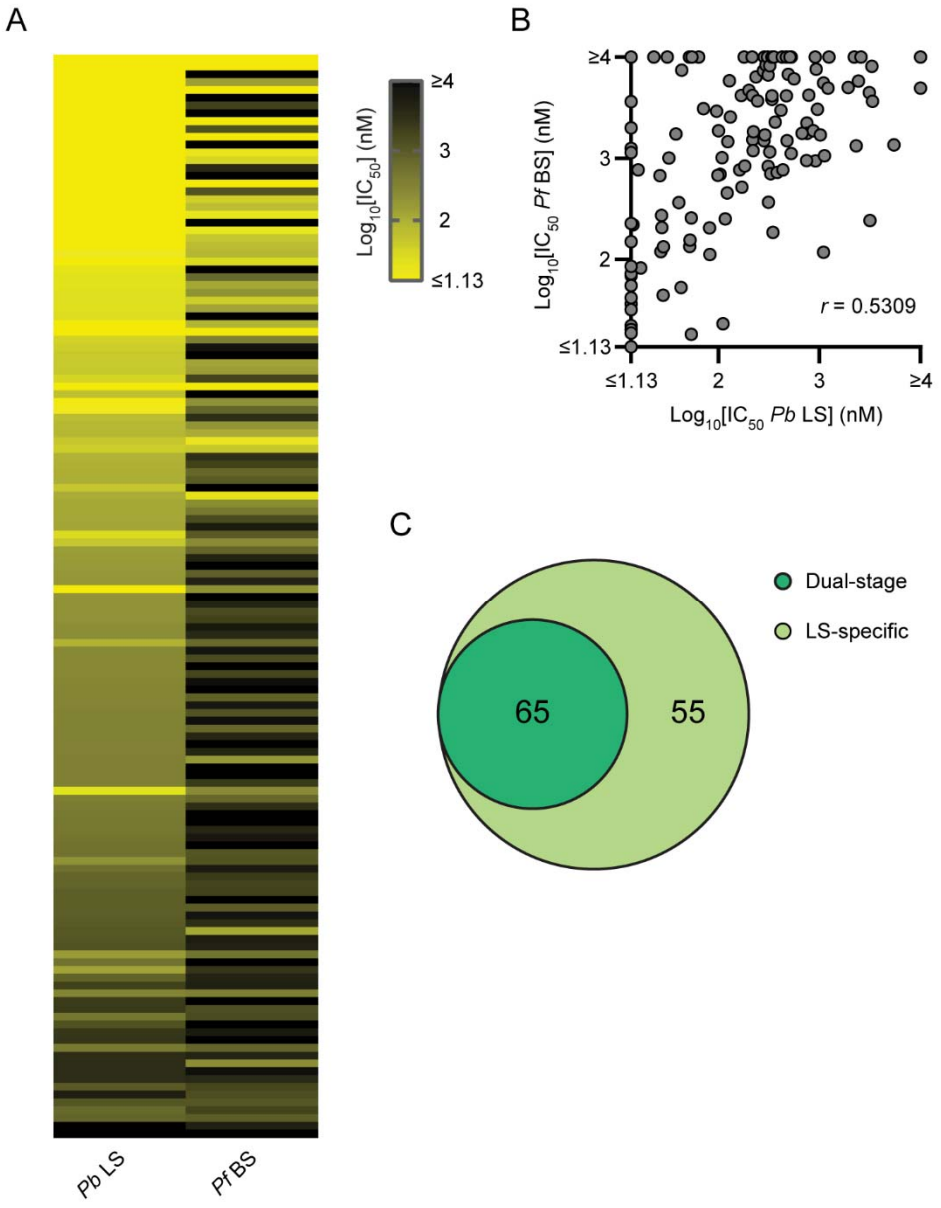
A
Log10[IC50] (nM)
≥4
3
2
≤1.13
Pb LS
Pf BS
B
Log10[IC50 Pf BS] (nM)
Log10[IC50 Pb LS] (nM)
r = 0.5309
≥4
3
2
≤1.13
C
Dual-stage
LS-specific
65
55

FIGURE 4.

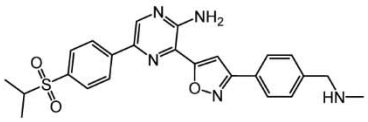

Hit # 14 (Berzosertib, VE-822)
ATR inh.
IC_{50} *Pb* LS: <13.6
IC_{50} *Pf* BS: 30.1 - 118.8

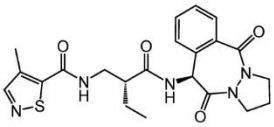

Hit # 19
SPPL2A inh.
IC_{50} *Pb* LS: <13.6
IC_{50} *Pf* BS: 33.1 - 49.5

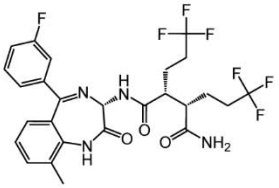

Hit # 24 (Varegacestat)
γ-secretase and pan-Notch inh.
IC_{50} *Pb* LS: <13.6
IC_{50} *Pf* BS: 18.5 - 446.0

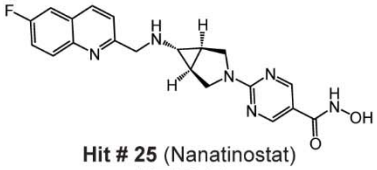

Hit # 25 (Nanatinostat)
HDAC inh.
IC_{50} *Pb* LS: <13.6 - 14.0
IC_{50} *Pf* BS: 49.2 - 105.8

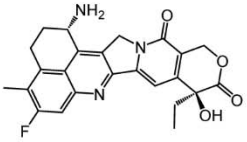

Hit # 26 (Exatecan)
DNA topoisomerase I inh.
IC_{50} *Pb* LS: <13.6 - 31.8
IC_{50} *Pf* BS: 68.1 - 82.0*

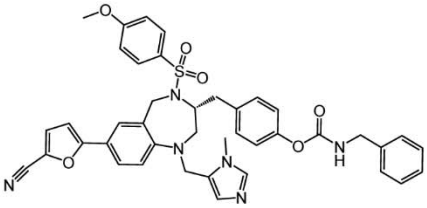

Hit # 30
RabGGTase inh.
IC_{50} *Pb* LS: 14.1 - 39.5
IC_{50} *Pf* BS: 110.0 - 130.4

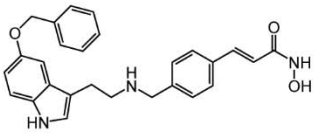

Hit # 31
HDAC inh.
IC_{50} *Pb* LS: 15.8 - 27.5*
IC_{50} *Pf* BS: 153.0 - 237.9*

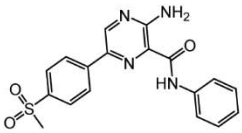

Hit # 37 (VE-821)
ATR inh.
IC_{50} *Pb* LS: 14.5 - 114.0
IC_{50} *Pf* BS: 115.2 - 460.1

FIGURE 5.

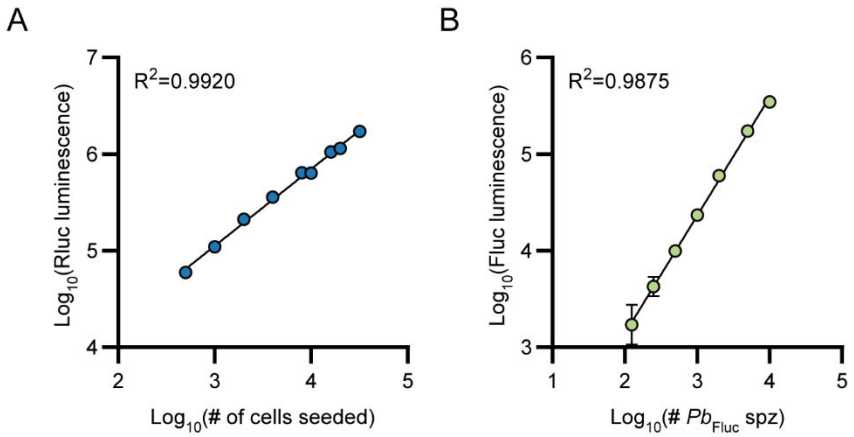
A
B
R2=0.9920
R2=0.9875
Log10(Rluc luminescence)
Log10(Fluc luminescence)
Log10(# of cells seeded)
Log10(# Pb Fluc spz)
7
6
5
4
3
2
1

FIGURE S1.

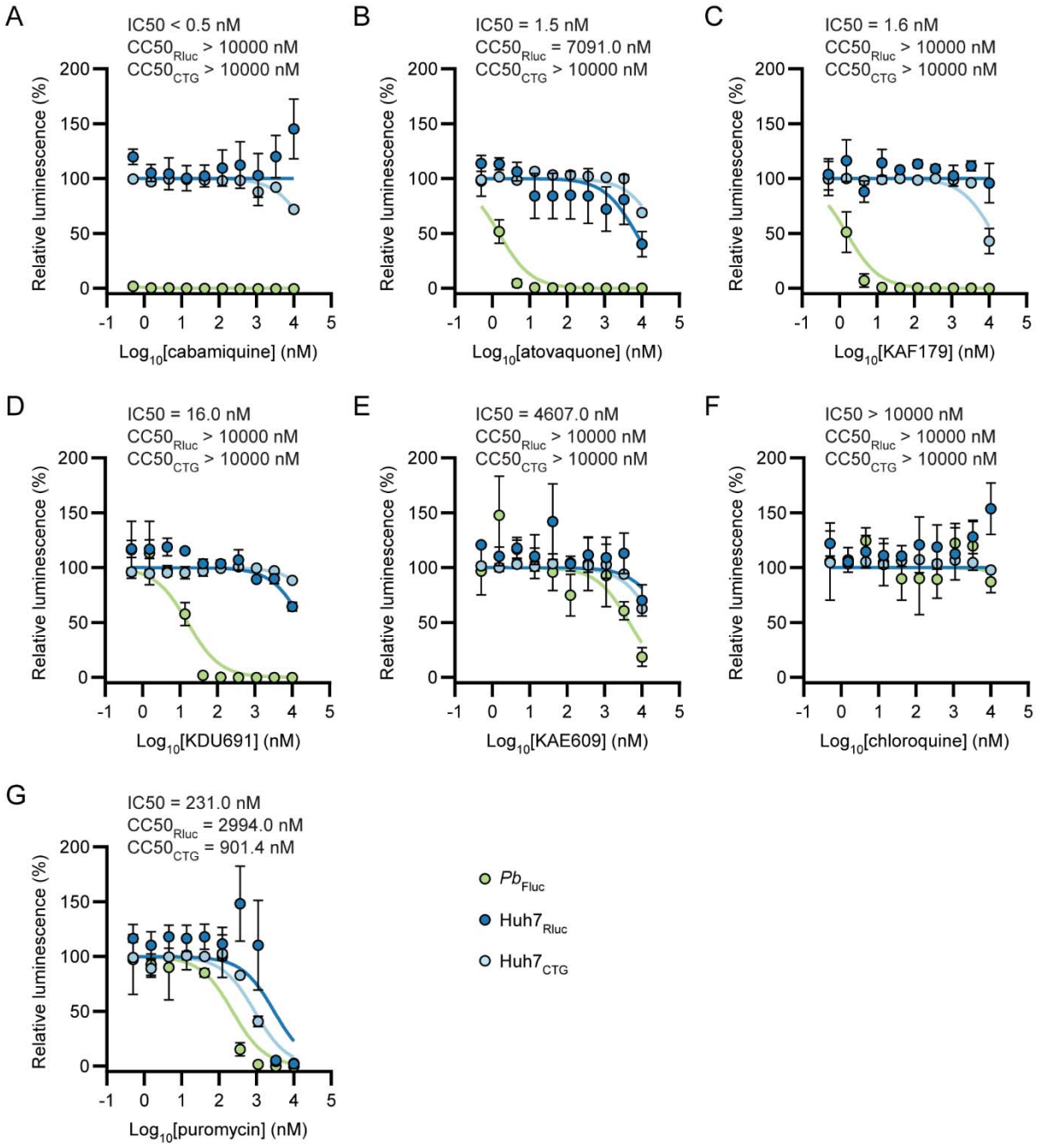
A
IC50 < 0.5 nM
CC50Rluc > 10000 nM
CC50CTG > 10000 nM
Log10[cabamiquine] (nM)
B
IC50 = 1.5 nM
CC50Rluc = 7091.0 nM
CC50CTG > 10000 nM
Log10[atovaquone] (nM)
C
IC50 = 1.6 nM
CC50Rluc > 10000 nM
CC50CTG > 10000 nM
Log10[KAF179] (nM)
D
IC50 = 16.0 nM
CC50Rluc > 10000 nM
CC50CTG > 10000 nM
Log10[KDU691] (nM)
E
IC50 = 4607.0 nM
CC50Rluc > 10000 nM
CC50CTG > 10000 nM
Log10[KAE609] (nM)
F
IC50 > 10000 nM
CC50Rluc > 10000 nM
CC50CTG > 10000 nM
Log10[chloroquine] (nM)
G
IC50 = 231.0 nM
CC50Rluc = 2994.0 nM
CC50CTG = 901.4 nM
Log10[puromycin] (nM)
Relative luminescence (%)
PbFluc
Huh7Rluc
Huh7CTG

FIGURE S2.

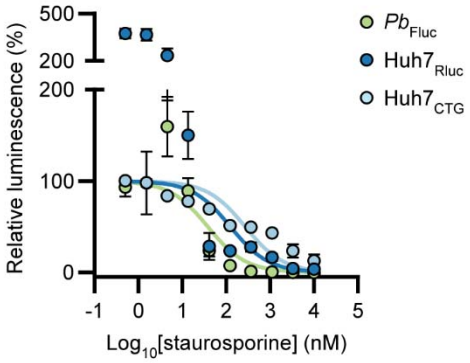
500
200
200
100
0
Relative luminescence (%)
-1
0
1
2
3
4
5
Log10[staurosporine] (nM)
Pb Fluc
Huh7 Rluc
Huh7 CTG

FIGURE S3.

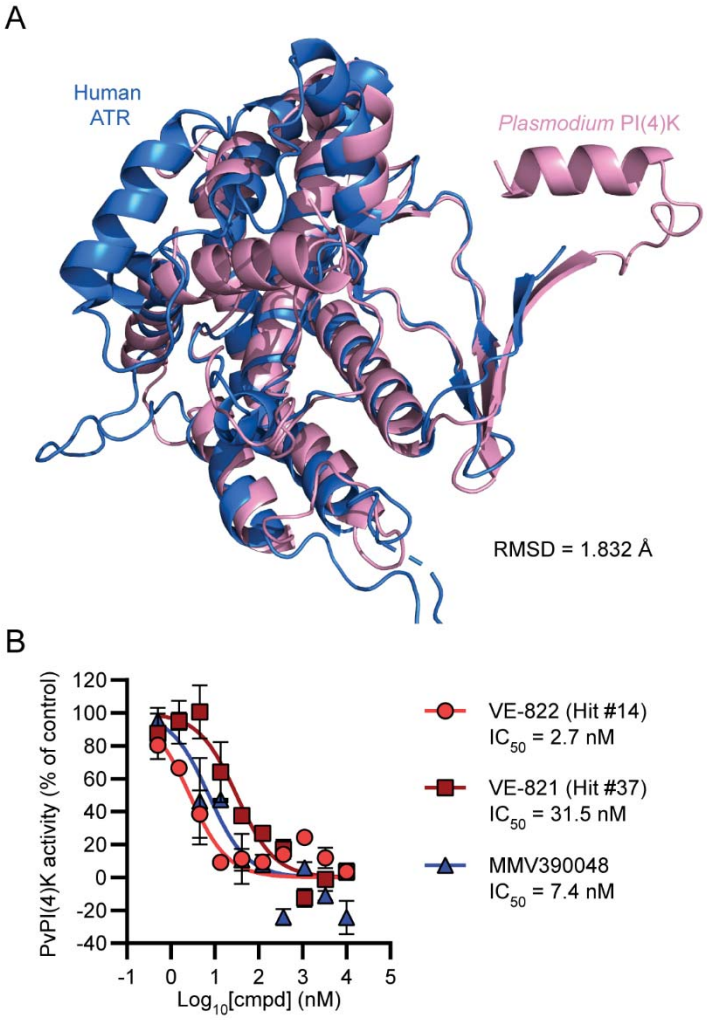
A
Human
ATR
Plasmodium PI(4)K
RMSD = 1.832 Å
B
PvPI(4)K activity (% of control)
120
100
80
60
40
20
0
-20
-40
-1
0
1
2
3
4
5
Log10[cmpd] (nM)
VE-822 (Hit #14)
IC50 = 2.7 nM
VE-821 (Hit #37)
IC50 = 31.5 nM
MMV390048
IC50 = 7.4 nM

FIGURE S4.